# Integrated cladding-pumped multicore few-mode erbium-doped fibre amplifier for space-division-multiplexed communications

H. Chen, C. Jin, B. Huang, N. K. Fontaine, R. Ryf, K. Shang, N. Grégoire, S. Morency, R.-J. Essiambre, G. Li, Y. Messaddeq and S. LaRochelle

*Nature Photonics* 10, 529-533 (2016)

Doi: 10.1038/nphoton.2016.125

# Integrated cladding-pumped multicore few-mode erbium-doped fibre amplifier for space-division multiplexed communications

H. Chen[1*], C. Jin[1,2], B. Huang[1,3], N. K. Fontaine[1], R. Ryf[1], K. Shang[1], N. Grégoire[2], S. Morency[2], R.-J. Essiambre[1], G. Li[3,4], Y. Messaddeq[2] and S. LaRochelle[2]

1 Nokia Bell Labs, 791 Holmdel Road, Holmdel, New Jersey 07733, USA.

2 Center for Optics, Photonics and Lasers, Université Laval, Québec G1V0A6, Canada.

3 CREOL, The College of Optics & Photonics, University of Central Florida, Orlando, Florida 32816, USA.

4 The College of Precision Instruments and Opto-electronic Engineering, Tianjin University, Tianjin 300072, China.

*e-mail: haoshuo.chen@nokia-bell-labs.com

**Abstract:**

Space-division multiplexing (SDM), whereby multiple spatial channels in multimode[1] and multicore[2] optical fibres are used to increase the total transmission capacity per fibre, is being investigated to avert a data capacity crunch[3,4] and reduce the cost per transmitted bit. With the number of channels employed in SDM transmission experiments continuing to rise, there is a requirement for integrated SDM components that are scalable. Here, we demonstrate a cladding-pumped SDM erbium-doped fibre amplifier (EDFA) that consists of six uncoupled multimode erbium-doped cores. Each core supports three spatial modes, which enables the EDFA to amplify a total of 18 spatial channels (six cores × three modes) simultaneously with a single pump diode and a complexity similar to a single-mode EDFA. The amplifier delivers >20 dBm total output power per core and <7 dB noise figure over the C-band. This cladding-pumped EDFA enables combined space-division and wavelength-division multiplexed transmission over multiple multimode fibre spans.

The bandwidth demands for optical networks are growing exponentially and will soon exceed the maximum achievable capacity of a single-mode fibre (SMF) due to fibre nonlinearities[4], resulting in a ‘capacity crunch’[3] in the near future. The simplest way to avert the ‘capacity crunch’ is to use multiple SMF transmission systems in parallel. However, this most basic form of SDM requires duplication of all the optical amplifiers, reconfigurable optical add–drop multiplexers and transponders for each additional fibre, and is subject to linear scaling of cost and complexity. Alternatively, SDM that uses the spatial

domain for integration can provide a similar capacity increase but with great potential for reducing the cost per bit of transmission. Examples include fibres with enlarged cores that support multiple spatial modes[1,5], fibres with multiple cores[2,6], wavelength switches that switch all cores/modes simultaneously[7] and optical fibre amplifiers[8,9].

In the past five years, tremendous progress has been made in both SDM components and SDM transmission. Spatial degrees of freedom have increased from 3 modes to 15 in few-mode fibres (FMFs) or multimode fibres (MMFs), and from 3 cores to 36 cores in multicore fibres (MCFs). Over 2 Pbit $s^{-1}$ transmission over 100 spatial channels in multimode MCFs[10,11] have been demonstrated. Different types of spatial multiplexers (SMUXs) based on bulk optics[12], fused fibre bundles[13], laser-inscribed three-dimensional waveguide devices[14] and photonic integration[15] have enabled efficient connections between multiple SMFs and SDM fibres. Efforts to reduce receiver computational complexity due to multiple-input-multiple-output (MIMO) processing include FMFs with low differential-group-modal-delay and low inter-mode group coupling[16,17] as well as MCFs with <–40 dB core-to-core crosstalk[18,19].

As for SDM optical amplifiers, core-pumped multimode and multicore EDFAs have previously been used for wavelength-division multiplexing (WDM)/SDM[20,21]. However, core pumping requires almost the same number of pump diodes as the number of cores, and offers only a slight reduction in complexity and costs compared to duplicating SMF amplifiers. Cladding-pumped amplifiers can significantly reduce the complexity and cost of multi spatial channel amplifiers[2,22-26]. Additionally, the gain for different modes can be simply balanced by employing uniform cladding pumping[27] instead of tailoring the pumping spatial mode content using multiple pumps in different modes[28] or incorporating complex doping profiles into the fibre design[29]. In cladding-pumped amplifiers, the pump light is coupled to the cladding modes independently from the core modes, which eliminates wavelength combining elements and also enables simple pumping schemes. For instance, side pumping[30] does not require access to the fibre facet, but instead couples pump light into the cladding modes through the side of the fibre (Supplementary Section ‘Side pumping’). The pump light illuminates all cores (Fig. 1a), eliminating the need for a separate pump diode per core. Moreover, uniform illumination of the cores simplifies modal gain equalization. The main drawback that has to be overcome with cladding-pumped amplifiers is the reduced pump power conversion efficiency, because the illuminated cladding area is much larger than the core area.

In this Letter, we explore integrated SDM optical amplifiers that can amplify many spatial channels and therefore significantly reduce the complexity and cost of SDM transmission systems. We have designed and fabricated an annular-cladding six-core erbium-doped fibre (EDF; Fig. 1b) to increase the pump power conversion efficiency. This work demonstrates amplification of 18 spatial channels (six cores with three spatial modes each) using only a single optical pump. The inner cladding is a depressed index region able to prevent pump light from entering the central region due to total internal reflection. This enhances the pump intensity around the cores in the annular cladding and can save more than 25% pump power compared to a uniform cladding (Supplementary Section 'Pump power for strong population inversion'), enabling a >20 dBm output power per core and <7 dB noise figure (NF) over the entire C-band (Supplementary Section 'Challenges in cladding-pumped EDFA'). This amplifier was then used in a 120 km WDM/SDM transmission experiment composed of three amplified spans.

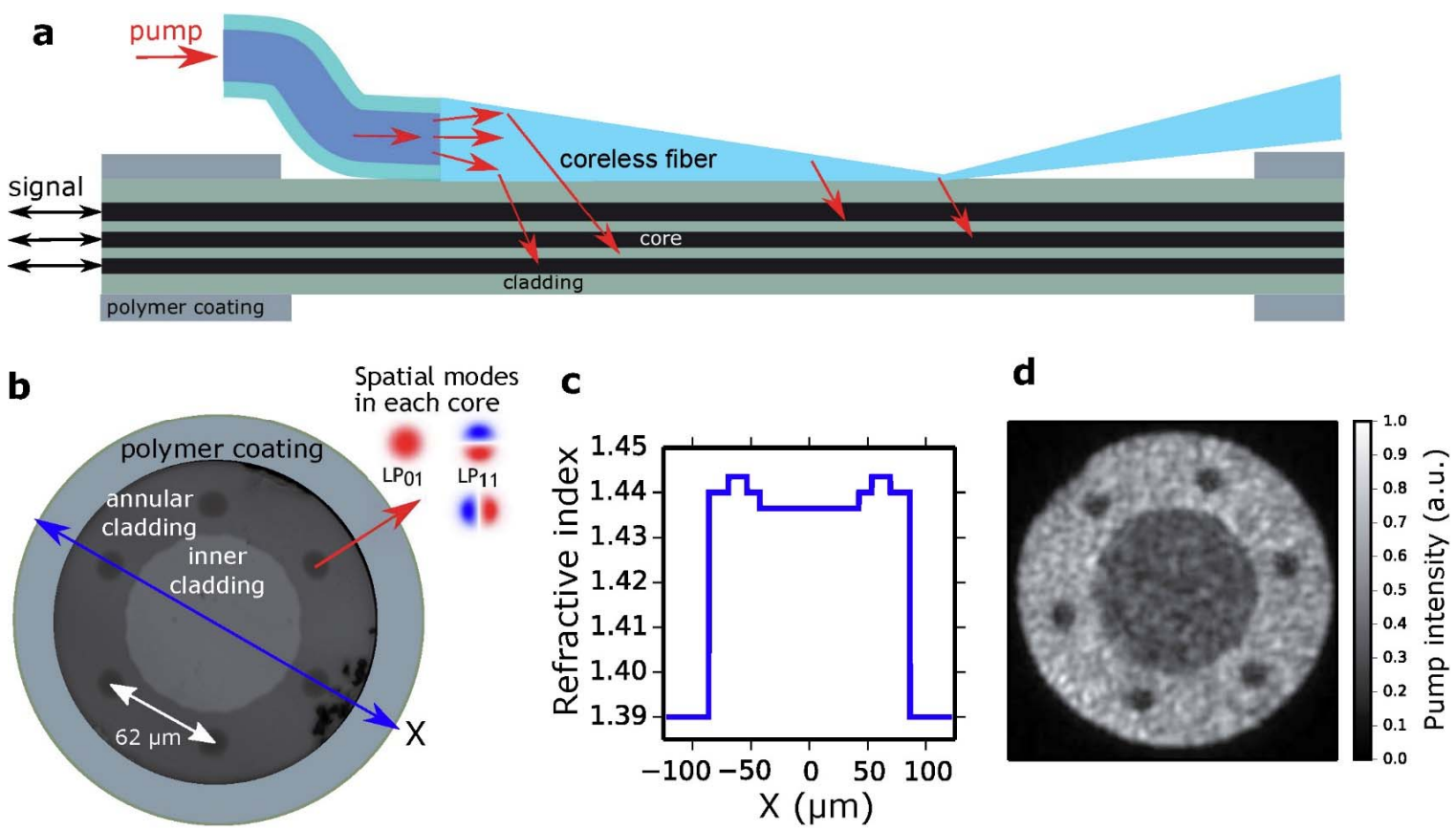


**Figure 1** | Cladding-pumped six-core EDFA. a, Schematics of side pumping. b, Image of EDF facet. c, Refractive index profile of EDF. d, Output pump intensity distribution with multimode side pumping at 980 nm.

The refractive index profile along the x axis (Fig. 1b) of the annular-cladding six-core EDF is presented in Fig. 1c. The fabrication of the six-core EDF is addressed in detail in Supplementary Section 'Fibre preparation and fabrication'. Each core supports the $LP_{01}$ mode and the two degenerated $LP_{11}$ modes in the C-band (Supplementary Section 'Fibre param-

eters'). To achieve high output power per spatial channel, which can only be accomplished if the EDFA maintains a high ratio of pump intensity to signal intensity throughout the gain medium so that it is not saturated, we designed core and cladding refractive indices to provide larger mode areas, thereby reducing the signal intensity without affecting the pump intensity. The calculated mode field areas are 168 and 179 $\mu m^2$ for the $LP_{01}$ and $LP_{11}$ mode groups, respectively, which are much larger than those of SMFs. The nearly identical mode fields also contribute to minimizing the mode-dependent gain, which was measured to be less than 2 dB (Supplementary Fig. 6c). We demonstrated that the average pump intensity in the annular cladding is enhanced by a factor of 1.45 compared to the inner cladding (Fig. 1d), which contributes to lower NFs through full population inversion at the input of the amplifier. It was verified that the annular cladding has negligible impact on the side-pump coupling efficiency, which is around 96%, similar to that of the uniform cladding (Supplementary Section 'Ray-tracing simulation').

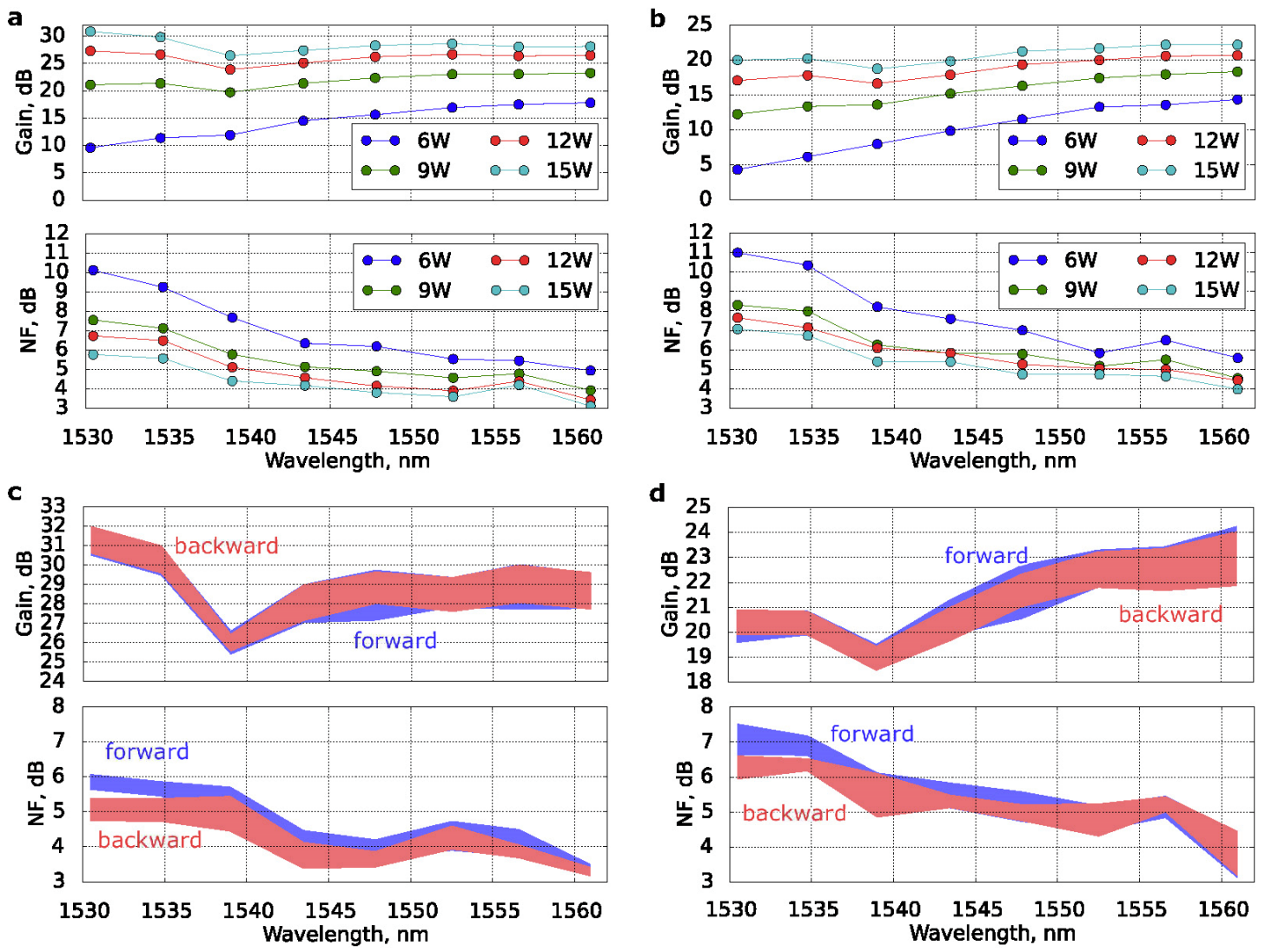


**Figure 2** | Internal gain and NF characterization. a,b, Results for $LP_{01}$ mode of one core in a forward-pumping configuration with a total input power of −12 and −2 dBm, respectively, as a function of coupled-pump power. c,d, Range of internal gains and NFs in both forwards and backwards pumping for all six cores with a total input power of −12 and −2 dBm, respectively.

Figure 2a,b shows the internal gains (excluding input and output coupling losses) and NFs for one of the six cores as a function of coupled-pump power in the forward-pumping configuration (Supplementary Section 'Gain and noise figure measurements'). Figure 2c,d shows the range of internal gains and NFs for all six cores with a coupled-pump power of 15 W and total input signal power of −12 and −2 dBm, respectively. The cladding-pumped six-core EDFA provides an output power of >20 dBm per core and <7 dB NF over the C-band for the $LP_{01}$ mode. Lower NFs at shorter wavelengths can be achieved by further increasing the pump intensity to saturate the amplifier less. The gain and NF deviations of 1 dB are mainly attributed to the inaccuracy in the measurements of input and output coupling losses. Performance discrepancies, especially for NFs at short wavelengths, can be observed between forward and backward pumping, which can be attributed to inadequate pump power for forward pumping at the input where the coreless fibre starts to be wrapped around the EDF. This slight deficiency can be eliminated by either using bidirectional pumping or by first coupling the pump into a passive fibre with an identical structure to the EDF. We replaced the SMF at the EDF output with a 50/125 μm MMF to detect the output power for all three spatial modes, as all the modes are excited at the same time, each with −2 dBm input power. It was measured that 22 dBm output power can be provided by each core with 15 W pump power coupled into the cladding.

To use each core as an independent amplifier, it is essential to have negligible core-to-core crosstalk and pump-depletion-induced crosstalk. The worst-case core-to-core crosstalk for a six-core EDFA spliced with two tapered fibre bundles was measured to be better than −35 dB, which is mainly attributed to fabrication errors in the tapered fibre bundles (Supplementary Section 'Crosstalk') and can be further minimized through fabrication optimization. The ratio between the single-core area and cladding area is 1.2%. A benefit of this small overlap of the gain medium with the pump is negligible pump depletion, which avoids pump-depletion-induced crosstalk. No pump-depletion-induced crosstalk was observed under different signal loading conditions (Supplementary Fig. 6c).

Figure 3a presents an overview of the multi-span FMF transmission experiment using the cladding-pumped six-core EDFA. The 120 km fibre link contains four graded-index FMF spans that support six spatial and polarization modes at 1,550 nm. The effective areas were 64 and 67 $\mu m^2$ for the $LP_{01}$ and $LP_{11}$ modes, respectively. The absorption was 0.226 dB $km^{-1}$ and the chromatic dispersion was 18.5 ps $nm^{-1}$ $km^{-1}$ at 1,550 nm. The different group delay varied from 60 to 140 ps $km^{-1}$ for different spans. Figure 3b depicts how all

six amplifying cores were used for either forward or backward transmission. In the forwards direction, a different core was used for amplification between the FMF spans (cores 1, 2 and 6). In the backwards direction, for the three remaining cores, dummy channels were launched to fully load the amplifier. The six FMFs of each fan-out were spliced to the FMF spans. The amplifier was operated with 8 W fibre-coupled power to compensate for the losses from the transmission FMF and the fan-outs.

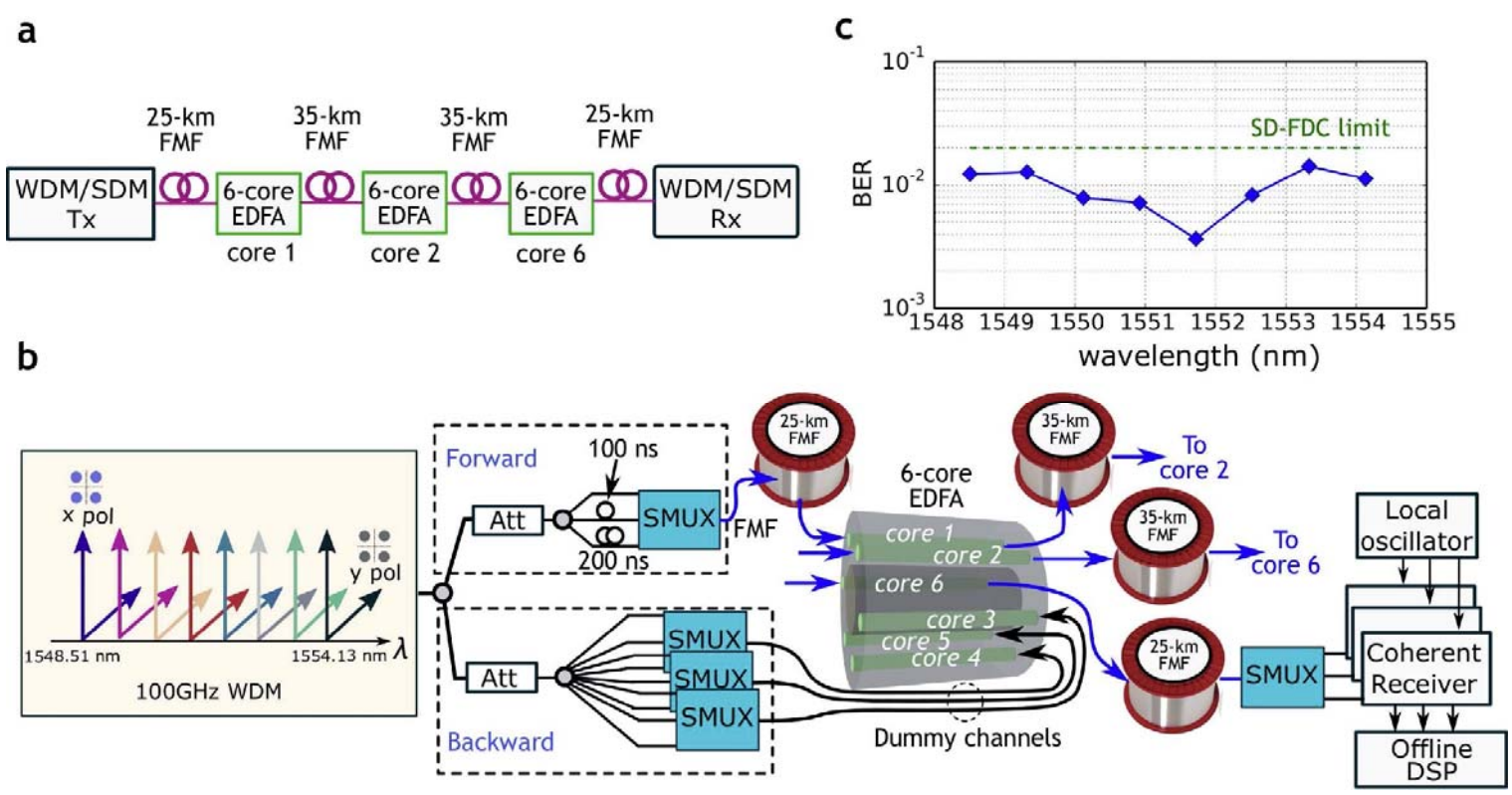


**Figure 3** | Multi-FMF span transmission. a, Overview of multi-FMF span with four FMFs and three amplifier units. b, The transmission set-up includes a WDM/SDM transmitter for generating signal and dummy channels, a 120 km transmission link with one in-line six-core EDF and a SDM receiver. c, BER for eight WDM channels.

The transmitter, which produced eight wavelengths spaced at 100 GHz, is illustrated in Fig. 3b. The even and odd wavelengths were separately modulated by independent 30 Gbaud quadrature phase shift keyed (QPSK) waveforms with Nyquist pulse shaping, and the WDM comb was then polarization multiplexed. Twelve independent launch signals were prepared by splitting and delay decorrelating the WDM comb and were coupled into the six spatial and polarization modes of the FMFs using mode-group selective photonic-lantern-based SMUXs. Optical attenuators were used to equalize the input signal power into each core. The combined SDM and WDM forward signal was transmitted through three cores of the amplifier over 35 km FMF after the first and second stage, and 25 km FMF after the transmitter and another 25 km FMF in front of the receiver. At the receiver, the forward SDM signals were demultiplexed by another photonic-lanternbased SMUX and fed to three polarization-diversity-multiplexed coherent receivers operating at 40 GS

$s^{-1}$. MIMO-based offline digital signal processing (DSP) was applied to recover the signals (Supplementary Section 'Data processing').

Figure 3c shows the bit-error rate (BER) curves for all wavelength channels averaged across all spatial modes after the 120 km FMF span, which are below the $2 \times 10^{-2}$ soft-decision forward error correction (SD-FEC) limit for all wavelengths with a net capacity of 2.4 Tb $s^{-1}$ assuming 20% overhead. After 120 km transmission, the optical-signal-to-noise ratio (OSNR) was larger than 17 dB (compared to the OSNR of 35 dB at the transmitter output), which provides an equivalent NF of 6 dB per core considering fibre losses and coupling losses (Supplementary Section 'Equivalent noise figure'). The transmission reach was constrained by the accumulated mode-dependent loss (MDL) around 26 dB, induced at each splicing point between the six-core EDF and the fan-in/fan-out due to mode-profile mismatch and pitch deviation after down-tapering (Supplementary Section 'Mode-dependent loss'). By optimizing the tapering parameters and using fibres with identical mode profiles, we should be able to minimize the accumulated MDL in addition to employing differential group delay-compensated FMF spans to increase the transmission reach.

This work presents a novel type of EDF capable of amplifying 18 spatial channels using both cores and modes, which is scalable to support a larger spatial channel count. More than 20 dBm total output power per core and <7 dB NF was achieved through cladding pumping, which can be an efficient and low-cost solution for integrated optical amplification. Increasing the number of guided modes for each core is an efficient means by which to increase the spatial channel counts within a limited cladding diameter, and negligible mode-dependent gain can be achieved by oversizing the core to support more modes than required[27]. The depressed index region is not limited to the centre and can be separated and distributed to any location of the cladding to enhance pump intensity. By increasing the refractive index contrast between the undepressed cladding region containing cores and the depressed index region, or by using an air hole for the depressed index region, the pump power conversion efficiency can be further enhanced. Future research needs to determine the maximum number of cores, the modes per core, and address the optimum ratio between core area and undepressed cladding area to maximize the pump conversion efficiency without inducing core-to-core pump-depletion-induced crosstalk.

## References


1. Ryf, R. *et al.* Mode-division multiplexing over 96 km of few-mode fiber using coherent 6 × 6 MIMO processing. *J. Lightw. Technol.* **30**, 521-531 (2012).
2. Sakaguchi, J. *et al.* 19-Core MCF transmission system using EDFA with shared core pumping coupled via free-space optics. *Opt. Express* **22**, 90-95 (2014).
3. Chralyvy, A. Plenary paper: the coming capacity crunch. *Proc. European Conf. Optical Communication* (ECOC) (2009).
4. Essiambre, R.-J., Kramer, G., Winzer, P. J., Foschini, G. J. & Goebel, B. Capacity limits of optical fiber networks. *J. Lightw. Technol.* **28**, 662-701 (2010).
5. Fontaine, N. K. *et al.* 30 × 30 MIMO transmission over 15 spatial modes. *Proc. Optical Fiber Communication Conf.* (OFC) Th5C.1 (2015).
6. Van Uden, R. G. H. *et al.* Ultra-high-density spatial division multiplexing with a few-mode multicore fibre. *Nature Photon.* **8**, 865-870 (2014).
7. Fontaine, N. K. *et al.* Heterogeneous space-division multiplexing and joint wavelength switching demonstration. *Proc. Optical Fiber Communication Conf.* (OFC) Th5C.5 (2015).
8. Jung, Y. *et al.* Cladding pumped few-mode EDFA for mode division multiplexed transmission. *Opt. Express* **22**, 29008-29013 (2014).
9. Jin, C., Ung, B., Messaddeq, Y. & LaRochelle, S. Annular-cladding erbium doped multicore fiber for SDM amplification. *Opt. Express* **23**, 29647-29659 (2015).
10. Sakaguchi, J. *et al.* Large spatial channel (36-core × 3 mode) heterogeneous few-mode multicore fiber. *J. Lightw. Technol.* **34**, 93-103 (2016).
11. Igarashi, K. *et al.* Ultra-dense spatial-division-multiplexed optical fiber transmission over 6-mode 19-core fibers. *Opt. Express* **24**, 10213-10231 (2016).
12. Klaus, W. *et al.* Free-space coupling optics for multicore fibers. *IEEE Photon. Technol. Lett.* **24**, 1902-1905 (2012).
13. Huang, B. *et al.* All-fiber mode-group-selective photonic lantern using graded-index multimode fibers. *Opt. Express* **23**, 224-234 (2015).
14. Chen, H. *et al.* Design constraints of photonic-lantern spatial multiplexer based on laser-inscribed 3-D waveguide technology. *J. Lightw. Technol.* **33**, 1147-1154 (2015).
15. Koonen, A. M. J., Chen, H., *et al.* Silicon photonic integrated mode multiplexer and demultiplexer. *IEEE Photon. Technol. Lett.* **24**, 1961-1964 (2012).
16. Gruner-Nielsen, L. *et al.* Few mode transmission fiber with low DGD, low mode coupling, and low loss. *J. Lightw. Technol.* **30**, 3693-3698 (2012).
17. Sillard, P., Bigot-Astruc, M. & Molin, D. Few-mode fibers for mode-division-multiplexed systems. *J. Lightw. Technol.* **32**, 2824-2829 (2014).
18. Hayashi, T., Taru, T., Shimakawa, O., Sasaki, T. & Sasaoka, E. Characterization of crosstalk in ultra-low-crosstalk multi-core fiber. *J. Lightw. Technol.* **30**, 583-589 (2012).
19. Imamura, K., Gonda, T. *et al.* 19-Core fiber with new core arrangement to realize low crosstalk. *Proc. OptoElectronics and Communication Conf.* (OECC) 312-313 (2014).

20. Ip, E. *et al.* 146λ × 6 × 19-Gbaud wavelength-and mode-division multiplexed transmission over 10 × 50-km spans of few-mode fiber with a gain-equalized few-mode EDFA. *J. Lightw. Technol.* **32**, 790-797 (2014).
21. Igarashi, K. *et al.* 110.9-Tbit/s SDM transmission over 6,370 km using a full C-band seven-core EDFA. *Opt. Express* **21**, 18053-18060 (2013).
22. Abedin, K. S. *et al.* Cladding-pumped erbium-doped multicore fiber amplifier. *Opt. Express* **20**, 20191-20200 (2012).
23. Takasaka, S. *et al.* Cladding-pumped seven-core EDFA using a multimode pump light coupler. *Proc. European Conf. and Exhibition on Optical Communication* (ECOC) We.4.A.5 (2013).
24. Ono, H. *et al.* 12-Core double-clad Er/Yb-doped fiber amplifier employing free-space coupling pump/signal combiner module. *Proc. European Conf. and Exhibition on Optical Communication* (ECOC) We.4.A.4 (2013).
25. Jain, S. *et al.* Few-mode multi-element fiber amplifier for mode division multiplexing. *Opt. Express* **22**, 29031-29036 (2014).
26. Chen, H. *et al.* Demonstration of cladding-pumped six-core erbium-doped fiber amplifier. *J. Lightw. Technol.* **34**, 1654-1660 (2016).
27. Fontaine, N. K. *et al.* Multi-mode optical fiber amplifier supporting over 10 spatial modes. *Proc. Optical Fiber Communication Conf.* (OFC) Th5A.4 (2016).
28. Bai, N., Ip, E., Wang, T. & Li, G. Multimode fiber amplifier with tunable modal gain using a reconfigurable multimode pump. *Opt. Express* **19**, 16601-16611 (2011).
29. Kang, Q. *et al.* Minimizing differential modal gain in cladding-pumped EDFAs supporting four and six mode groups. *Opt. Express* **22**, 21499-21507 (2014).
30. Theeg, T., Sayinc, H., Neumann, J. *et al.* Pump and signal combiner for bi-directional pumping of all-fiber lasers and amplifiers. *Opt. Express* **20**, 28125–28141 (2012).

## Acknowledgements

This work was supported in part by the ICT R&D program of MSIP/IITP, Republic of Korea (R0101-15-0071, 'Research of mode-division-multiplexing optical transmission technology over 10 km multimode fibre'), by the National Basic Research Program of China (973, project no. 2014CB340103/4), by the Canada Research Chair in Advanced Photonics Technologies for Communications (APTEC), by the Canada Excellence Research Chair in Enabling Photonic Innovations for Information and Communications (CERCP) and the Natural Sciences and Engineering Research Council of Canada (NSERC), and by NSFC Projects 61377076, 61307085 and 61335005. The authors acknowledge OFS Labs for the few-mode fibre. The authors also thank R.W. Tkach and P.J. Winzer for support and valuable discussions.

## Author contributions

H.C. and C.J. developed the concept. C.J. and S.L. designed the fibre. N.G., S.M. and Y.M. fabricated the fibre. H.C., C.J., B.H. and K.S. conducted the fibre amplifier characterization. H.C. and C.J. conducted the ray tracing simulation. H.C., B.H. and N.K.F. fabricated the fan-in/fan-out. H.C., N.K.F. and R.R. conducted the transmission experiments. H.C. and N.K.F. wrote the manuscript. R.-J.E., G.L., Y.M. and S.L. helped write the article and provided funding.

**DOI: 10.1038/NPHOTON.2016.125**

# Supplementary information

## Pump power for strong population inversion

Low noise figure (NF) and high gain can only be obtained through strong population inversion. In the absence of an input signal and neglecting amplified spontaneous emission in a short fibre segment, the required pump power to achieve an inversion ratio of $\eta$ can be calculated as[1]: $P = \eta[(h\nu A_{21}/\sigma_{13})A_{clad}]/(1-\eta)$, where $h$ is the Planck's constant, $\nu$ is the pump light frequency, $A_{21} = 100$ $s^{-1}$ is the spontaneous emission rate, $\sigma_{13} = 2.18 \times 10^{-25}$ $m^2$ is the pump absorption cross section at v (corresponding to 980 nm), $A_{clad}$ is cladding area over which the pump is distributed.

A low NF requires a population inversion > 90%[1,2]. For an optical fibre with the pump power uniformly distributed in a cladding with a diameter of 170 μm, this low NF constraint requires approximately 18 W of pump power. For the designed annular-cladding 6-core erbium-doped fibre (EDF) with an inner cladding diameter of 85 μm, the required pump power is reduced to 13 W.

## Challenges in cladding-pumped EDFA

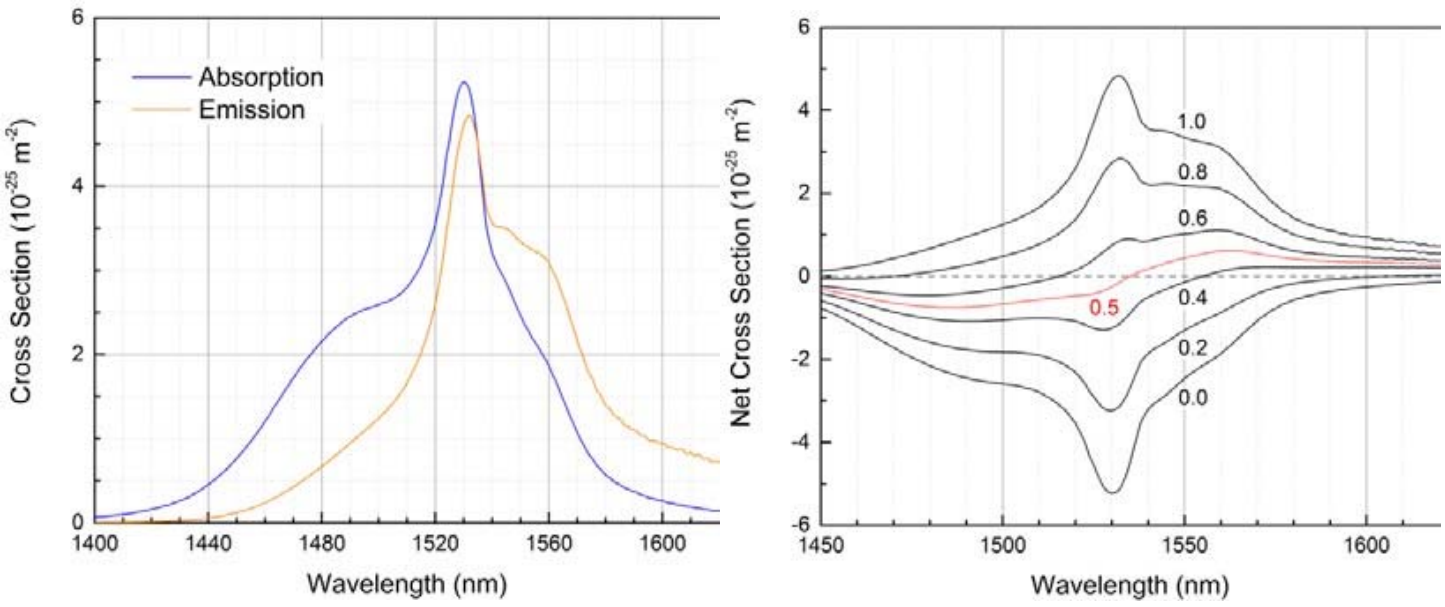


(a) (b)

**Supplementary Figure 1**| a, absorption and emission cross sections of erbium ions for the fabricated 6-core EDF. b, net cross section of erbium ions for the fabricated EDF under different inversion ratios.

The gain shape of the EDFA is determined by the shape of the absorption, $\sigma_a$, and emission, $\sigma_e$, cross sections of erbium ions as shown in Supplementary Figure 1a. Since the pump light is spread across the entire cladding in cladding pumped amplifiers, the pump intensity becomes relatively

weak, which makes it more challenging to fully invert the gain medium. The gain shape for different levels of population inversion is shown in Supplementary Figure 1b. It can be observed that low inversion results in gain shift towards L-band. Therefore only strong population inversion (>0.6) can produce high gain and low NFs in the C-band[3,4].

**Side pumping**

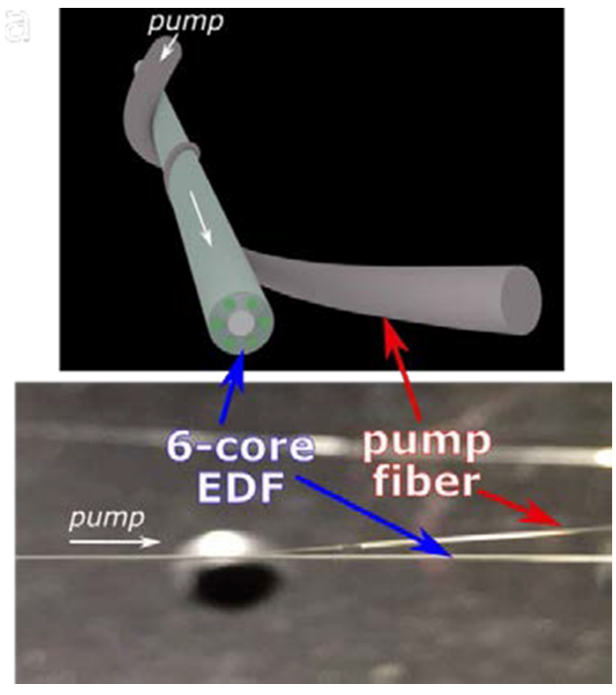


**Supplementary Figure 2**| Schematic and image of the side-pump coupling technique using a tapered coreless fibre.

Side pumping injects the pump light into the inner cladding using either embedded mirrors[5], V-grooves[6], a downsized capillaries[7] or down-tapered fibres[8]. Supplementary Figure 2 illustrates the side-pump coupling combiner using a down-tapered coreless fibre wrapped on a double-cladding erbium doped multicore fibre[9]. In the experiments, a commercially available high power 980nm laser diode with a 105/125-µm (core diameter/cladding diameter) multimode fibre (MMF) pigtail was used as the pump source. It produces an out-put power up to 25 W and has a wavelength temperature drift < 0.3 nm·°C$^{-1}$ and a spectral full width at half maximum < 3 nm. The MMF has a numerical aperture (NA) of 0.22 and was spliced to a 125-µm diameter coreless fibre. The coreless fibre was tapered down to a diameter of 15 µm over a length of 20 mm and wrapped 1.5 times around a 50 mm section of uncoated EDF. A tension was applied to bring both fibres in physical contact on the pump side. After the coupling area, an air gap between the pump delivery fibre and the EDF prevents the pump light from coupling out of the EDF. Along the taper, the light is adiabatically transferred from the tapered fibre into the amplifying fibre. An efficiency around 65% was achieved, which could be improved to 90%[8] by tapering down the coreless fibre to a smaller diameter (5 to 10 µm) and by fusing the down-tapered coreless fibre with the EDF to enhance physical contact.

## Fibre preparation and fabrication

Silica optical fibre preforms are usually fabricated by vapor-phase techniques that can be broadly classified into two categories, namely inside and outside deposition. The former includes modified chemical vapor deposition (MCVD)[10] and plasma chemical vapor deposition (PCVD)[11], while the later encompasses vapor axial deposition (VAD)[12] and outside vapor deposition (OVD)[13]. Rare-earth element doping in the preform can be achieved either in vapor-phase or in liquid-phase. Among the liquid-phase techniques, solution doping[14] is a convenient process.

In this letter, we used a standard MCVD process for silica glass deposition of the fibre waveguide structure and solution doping for loading erbium ions into the fibre core with a typical concentration of $2.8 \times 10^{25}$ ions/$m^3$. The speed and temperature of the MCVD process was optimized to control the porosity of the deposited soot, see reference[15]. The multicore EDF was subsequently fabricated from the single-core preform by a stack-and-draw method, which is widely employed for microstructure[16] or photonic crystal fibre fabrication[17]. The preform deposition, stack assembly and fibre drawing were all done at the Centre for optics, photonics and lasers (COPL) of Université Laval. Additional details on the process steps are given below.

Initially, silicon chloride ($SiCl_4$) gas incorporated in a mixture of oxygen and helium is blown through a pure silica substrate tube and heated by an oxy-hydrogen flame. Oxidation, as written in Equation (1), under this high temperature condition leads to silicon dioxide deposition on the internal surface of the support tube resulting in the so-called soot boule.

$$SiCl_4 + O_2 = SiO_2 + 2Cl_2 \quad (1)$$

Note that the torch temperature to obtain soot boule should be less than about 1500 °C to avoid verification, i.e. sintered glass deposition inside the silica tube that typically occurs under higher temperatures of about 1800-2000 °C. The silica soot, that finally covers all the inside surface of the pure silica tube substrate, has a porous structure with pore diameters that can be varied from nm to µm scale[18]. Although we have not measured the porosity of the soot, t is sufficiently repeatable to meet the need of our multicore design. By care-fully adjusting the input flow rate of the gas mixture and the substrate tube temperature, one can control the density of the soot structure to achieve the designed distribution profile of erbium ions.

Next, the tube with the deposited silica soot was immersed into a deionized water based solution that comprises both erbium chloride [$ErCl_3$-6($H_20$), in which erbium exists in the form of ions] and aluminum chloride [$AlCl_3$-6($H_20$)] crystalline hydrate. Erbium ion loading was thus performed by

capillary action[19]. We prepared the solution to achieve desired erbium ion doping concentration in the fibre, which depends on both the density of silica soot and the erbium ion concentration of the solution[14]. Afterwards, the tubes with the doped soot boules were dried with nitrogen to remove the aqueous solution.

After doping, the tube with the soot boule was put back on the lathe to complete the process. It was firstly dehydrated by oxy-hydrogen torch heating at low temperature. An oxidation reaction, as expressed in Equations (2) and (3), also occurs during this step and, consequently, all the dopants were transformed within the soot boule in the form of oxides. Secondly, vitrification of the soot structure was carried out under torch temperature about 2000 °C. Thirdly, extra torch heating collapses the doped tube into a solid glass preform rod with a diameter of around 15 mm.

$$4ErCl_3 + 3O_2 = 2Er_2O_3 + 6Cl_2 \quad (2)$$

$$4AlCl_3 + 3O_2 = 2Al_2O_3 + 6Cl_2 \quad (3)$$

Since the doped multicore fibre has six cores, in order to achieve sufficient fibre length, we made three identical doped silica preforms using the process described above. Supplementary Figure 3 shows the refractive index profile (refractive index) for all the three pre-forms (measured by Photon Kinetics PK2600). The preforms were subsequently cut in half so that each preform was used for two of the cores.

To make the stack assembly, the outside diameter of the preforms must be reduced. The three fabricated doped single core preforms were therefore etched, via soaking into HF acid solution, to a diameter of about 2.9 mm. During the HF etching, the core dimension is not modified. The stack assembly also requires a low index fluorine doped silica rod to make the inner cladding. This rod was similarly fabricated by the MCVD deposition, vitrification and collapse process described above by mixing fluorine with the silicon chloride gas. This rod is coreless and undoped with erbium. The lower index fluorine rod was placed at the center of a pure silica holding tube with external and internal diameter of 18 mm and 16 mm, respectively. Then, six doped core rods were stacked around and apart from the fluorine-doped silica rod in a hexagonal packing configuration. Additionally, we used pure silica rods to fill the empty space and to fix the core-spacing and core-to-cladding distances. These silica rods make the annular cladding that guides the pump. The bundle was hold in place by welding a 20-mm long and 15-mm wide silica rod on the bottom of the stacked preform. Supplementary Figure 4 illustrates the image of stacked preform transverse cross-section. Finally, the stacked preform was drawn to 177-µm fibre diameter and coated with

a lower index polymer to make the final double-clad multi-core doped fibre. During drawing, the fibre is further over coated with a higher index polymer to maintain the fibre mechanical properties.

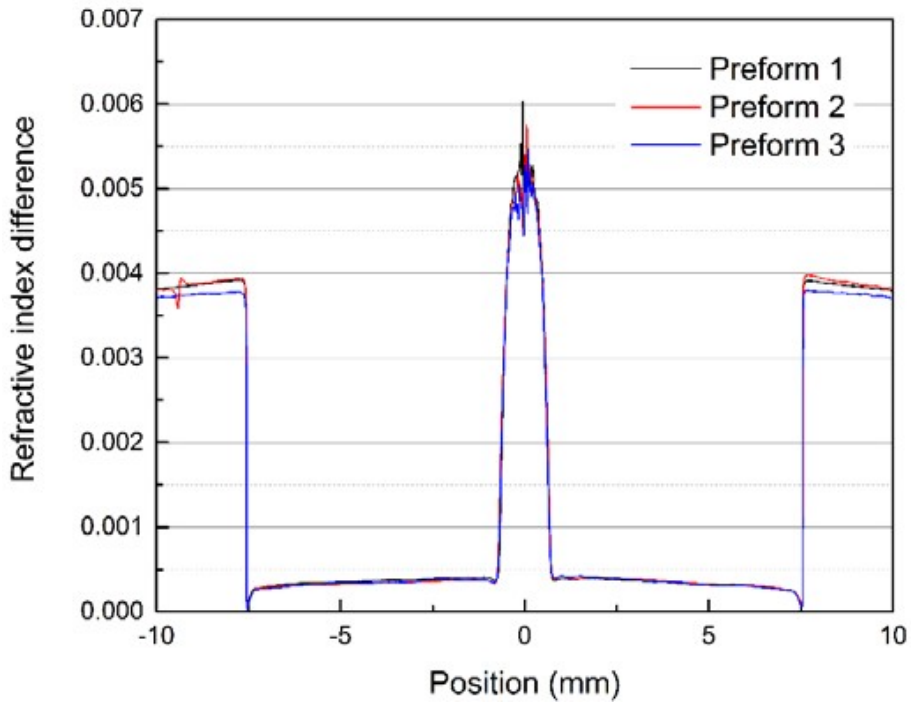


**Supplementary Figure 3**| Refractive index difference profile of the three doped core single preforms.

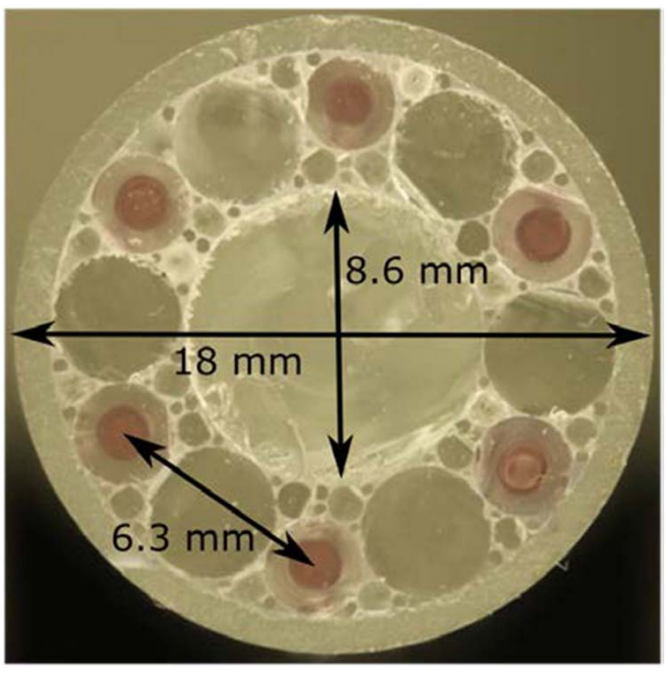


**Supplementary Figure 4**| Stacked preform (assembly) transverse cross-section image. In the figure, the six rods with 'red' centers are the doped cores. The largest rod at center is fluorine-doped silica inner cladding and the rest of the area is filled with pure silica rods of different sizes.

**Fibre parameters**

Each core of the 6-core EDF has a numerical aperture (NA) of 0.104 and a diameter of 16.5 µm. The core-to-core pitch is 62 µm. The low-index inner cladding at the center is made of fluorine-

doped silica that creates a refractive index step of $6 \times 10^{-3}$ compared to the index of the annular cladding populated by the six cores. The whole cladding diameter is 170 µm, while the inner cladding diameter is 85 µm. The edges of the cores are placed 10 µm from the annular cladding inner boundary and 16 µm from the outer boundary, respectively. A low-index polymer coating with a numerical aperture (NA) of 0.4 acts as a double cladding to confine the cladding modes in the annular glass cladding. The NA between the annular cladding and inner central cladding is 0.11.

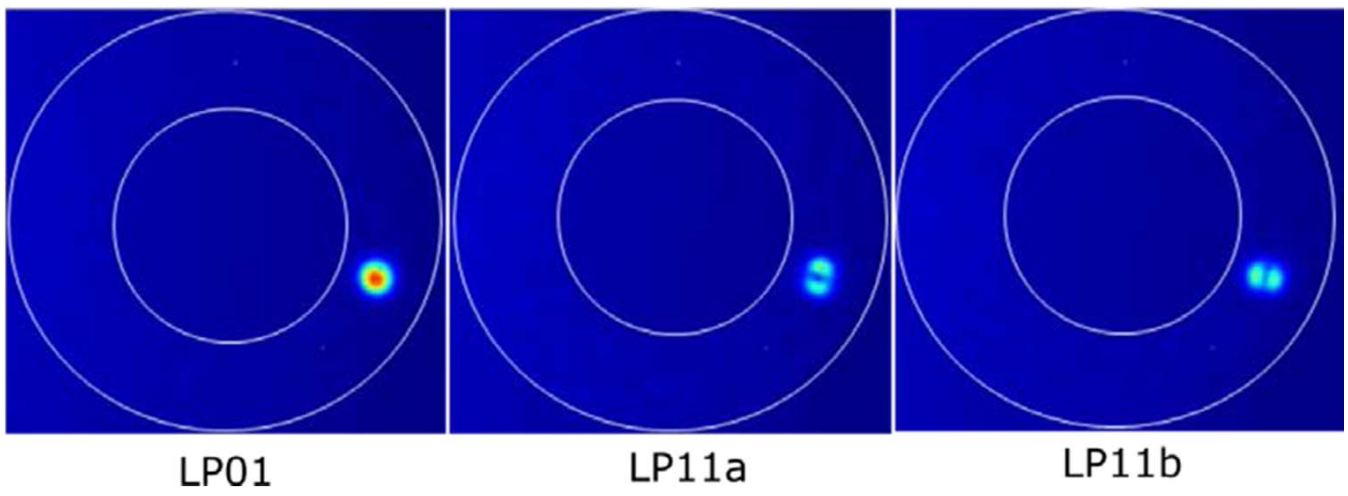


**Supplementary Figure 5**| Three individually excited spatial modes at 1300 nm.

The mode profiles of the three spatial modes guided by one of the six cores are shown in Supplementary Figure 5 using a mode-selective photonic lantern at 1300 nm to individually excite each mode. Erbium ions have negligible absorption at 1300 nm, which makes it possible to observe sharp images of excited modes.

**Ray-tracing simulation**

We used ray-tracing implemented in ZEMAX to simulate the side-pump coupling efficiency, and the pump confinement for two cladding structures: uniform and annular clad-ding. $10^7$ rays were launched into the coreless fibre from a source at the input facet with the same NA as the MMF used in the measurements. The detectors were placed at the end of both fibres and the pump power distribution was calculated by counting the number of rays exiting the transverse cross section.

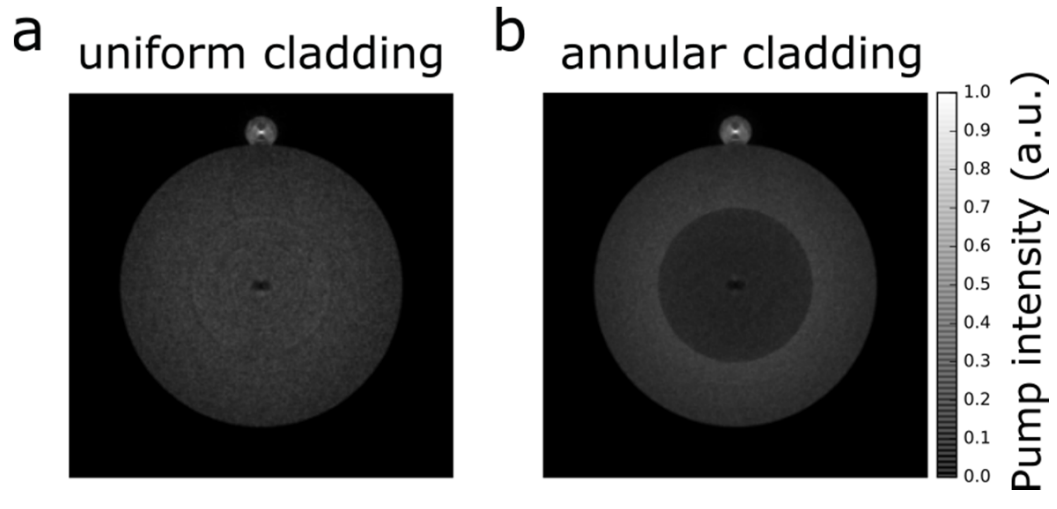


**Supplementary Figure 6**| Simulated pump power distribution for uniform and annular cladding by side pumping.

Supplementary Figure 6 shows the simulated pump power distribution for uniform and annular cladding, respectively, by side pumping.

**Gain and noise figure measurements**

The gain and NF performance of each EDF core was characterized in the wavelength-division multiplexing (WDM) configuration using 8 laser sources covering the C-band as the signal and an optical spectrum analyzer (OSA) to measure the output spectrum. The input signal power was adjusted by a variable optical attenuator. The SMFs at the input and out-put are placed on two 3-axis stages and were butt-coupled onto each core of a 2.1-m long 6-core EDF to selectively excite and detect the $LP_{01}$ mode with a mode extinction ratio larger than 30 dB. The input and output sections of the EDF were fixed on two fibre holders. Two isolators at the input and output were used to prevent lasing induced by facet reflection. Switching the input and output SMFs enabled characterization of the EDFA under both forward and backward pumping. With the pump coupling efficiency of 65%, the maximum coupled-pump power is 15 W. Any residual cladding pump was dumped via a cladding pump light stripper made by degrading the fibre surface through HF etching. A mental cover attached to a heat sink can be used to cover the pump stripper to avoid physical damage in practical applications. Due to the degeneracy of two $LP_{11}$ modes, it is difficult to accurately characterize each $LP_{11}$ mode in terms of NF. The NF of both $LP_{11}$ modes is expected to be similar.

**Crosstalk**

To investigate core-to-core and pump-depletion-induced crosstalk, the EDF was characterized using fibre fan-in/fan-out and the setup is illustrated in Supplementary Figure 7a. Supplementary Figure 7b shows the schematic and facet image of the fan-in/fan-out based on a tapered fibre

bundle that consists of 6 graded-index cores with a diameter of 15 µm arranged in a ring to match the core structure of the 6-core EDF with a core-to-core pitch of 62 µm. The input few-mode fibres (FMFs) of the fan-in/fan-out device support 15 spatial modes and are spliced to other FMFs supporting 3 spatial modes with coupling losses from the $LP_{01}$ to $LP_{01}$ and $LP_{11}$ to $LP_{11}$ are < 0.5 dB. Mode-group selective photonic-lantern-based spatial multiplexers (SMUXs)[20,21] with a mode selectivity better than 12 dB excite the three spatial modes with 0.5-dB loss for the $LP_{01}$ and 1.5-dB loss for the $LP_{11}$ modes, respectively.

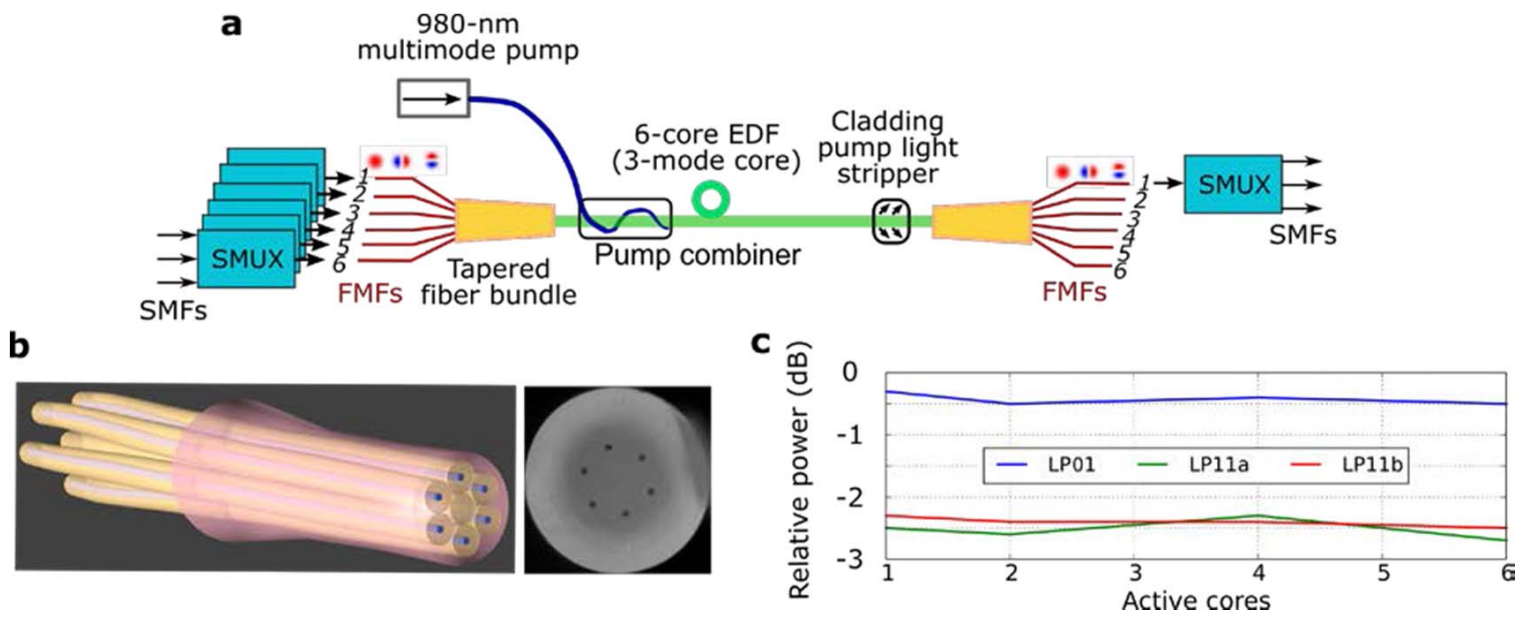


**Supplementary Figure 7**| Core-to-core crosstalk and pump-depletion-induced crosstalk characterization. a, Characterization setup for the cladding-pumped 6-core EDF with connected fan-in/fan-outs. b, Schematics and facet image of a tapered-fibre-bundle-based fan-in/fan-out. c, Output power per mode under different signal loading conditions.

Supplementary Figure 7c shows the amplifier output power per spatial channel of one core under different signal loading conditions in saturation condition.

**Data processing**

Off-line digital signal processing was applied to recover the signals and the preprocessing steps include: 2 × resampling, front-end skew corrections, chromatic dispersion and frequency offset correction. A 6 × 6 (6 = 3 spatial modes × 2 polarizations) frequency-domain equalizer with 800 symbol-spaced taps based on a data-aided least-mean-square (LMS) algorithm was applied to converge the equalizer and determine the channel impulse response. For bit-error rate counting, we used the constant-modulo algorithm (CMA) to slowly adapt the equalizer followed by carrier-phase recovery.

**Equivalent noise figure**

It has been verified in both simulation and measurement that the performance of few-mode multi-span transmission is not determined by the mode-dependent NF of the EDFA but the overall amplified spontaneous emission (ASE)[22]. In order to evaluate the performance for the cascaded amplification case, system noise figure $NF_{sys}(dB) = SNR_{in}(dB) - SNR_{out}(dB)$ and effective noise figure $NF_{eff}(dB) = NF_{sys}(dB) - 10 \times \log_{10}(m) - \alpha(dB)$ were used, where $SNR_{in}(dB)$ is the overall input signal-to-noise ratio in dB for the modes, $SNR_{out}(dB)$ is the overall output signal-to-noise ratio in dB for the modes, m is the number of amplifiers in a chain and $\alpha(dB)$ is the fibre span loss.

**Mode-dependent loss (MDL)**

The total 26-dB MDL can be broken down as: 1) 3-dB MDL at each splicing point between the 6-core EDF and fan-in/fan-out × 6, 2) 2-dB mode-dependent gain × 3 and 3) 2-dB MDL from two space multiplexers (SMUX). Mode-dependent loss (MDL) can be varied across the frequency. A frequency-averaged MDL was applied and calculated based on the con-verged equalizer acquired in the digital signal processing. The equalizer can be represented in frequency domain by a matrix $H_f$ with a size of $N_m \times N_m \times L_b$ , where $N_m$ is the number of space-polarization modes and $L_b$ is the equalizer length in number of taps ($N_m = 6$ and $L_b = 1024$ in our case). The last dimension of $H_f$ corresponds to different frequencies. Therefore, at each frequency, the equalizer is a 2-dimensional $N_m \times N_m$ matrix written as $H_{fi}$, where i is from 1 to $L_b$. $N_m$ singular values for each frequency were calculated by applying singular value decomposition to each $H_{fi}$. The frequency-averaged MDL was calculated based on the square of $N_m$ averaged singular values $S_j$ over the frequency, where j is from 1 to $N_m$ through application of $MDL = 10 \times \log_{10}[\max(S_j^2)/\min(S_j^2)]$.

Supplementary Figure 8 gives the intensity-impulse response $|h|^2$ after 120-km transmission averaged over all 6 × 6 spatial channels through application of $|h|^2=\sum\sum|h_t|^2$, where $h_t$ is the Fourier transform of $H_f$ . Multiple peaks from coupling between $LP_{01}$ and $LP_{11}$ modes at the 6 splice points can be observed in Supplementary Figure 8. Supplementary Figure 9 provides the BER for each spatial and polarization mode versus wavelength. There are four spatial and polarization modes in the $LP_{11}$ mode group and two in the $LP_{01}$ mode group. Lower BERs were achieved for the $LP_{01}$ modes since they are less sensitive to the errors at each splicing point compared to the $LP_{11}$ modes.

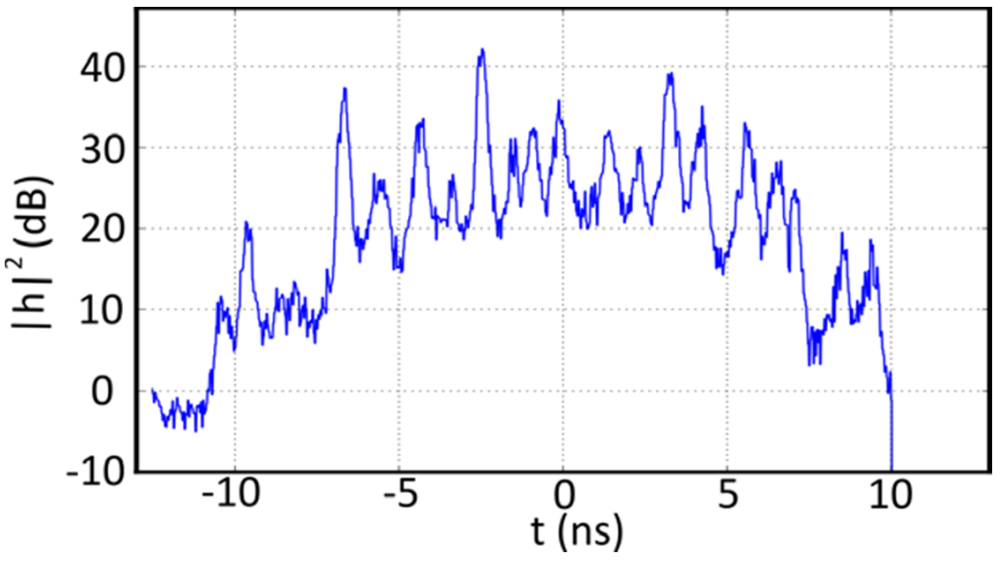


**Supplementary Figure 8**| Intensity-impulse response.

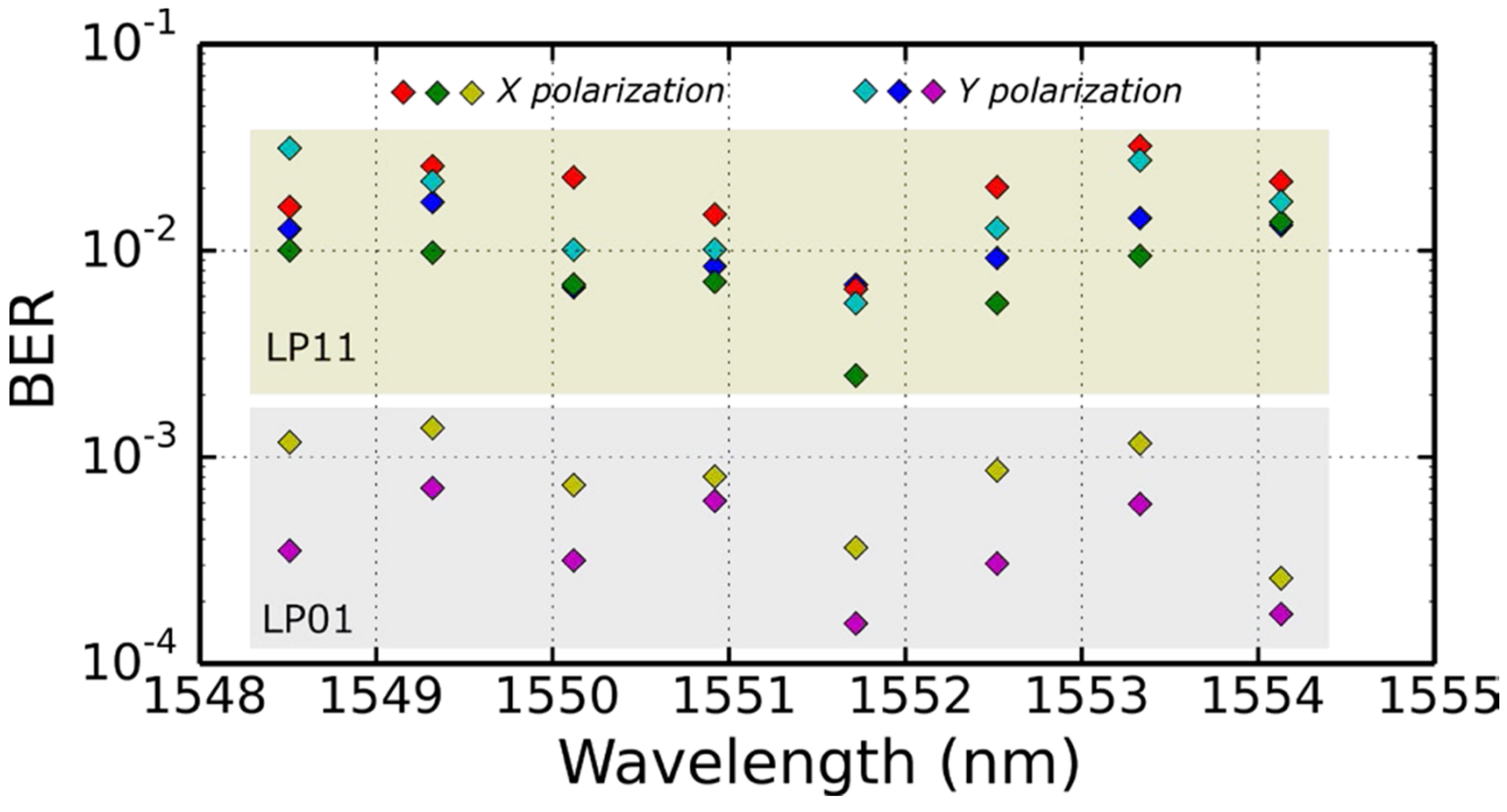


**Supplementary Figure 9**| BER for each spatial and polarization mode versus wavelength.

## References


1. Krummrich, P. M. & Petermann, K. Evaluation of potential optical amplifier concepts for coherent mode multiplexing. in *Optical Fibre Communication Conference and Exposition* (OFC/NFOEC), 2011 and the *National Fibre Optic Engineers Conference* OMH5 (2011).

2. Jin, C., Ung, B., Messaddeq, Y. & LaRochelle, S. Annular-cladding erbium doped multi-core fibre for SDM amplification. *Opt. Express* **23**, 29647 (2015).

3. Söderlund, M., Tammela, S., Pöyhönen, P., Leppihalme, M. & Peyghambarian, N. Amplified spontaneous emission in cladding-pumped L-band erbium-doped fibre amplifiers. *Photonics Technol. Lett. IEEE* **13**, 22-24 (2001).

4. Takeshima, K. et al. 51.1-Tbit/s MCF Transmission over 2,520 km Using Cladding Pumped 7-core EDFAs. in *Optical Fibre Communication Conference* W3G-1 (2015).

5. Koplow, J. P., Moore, S. W. & Kliner, D. A. V. A new method for side pumping of double-clad fibre sources. *IEEE J. Quantum Electron.* **39**, 529-540 (2003).

6. Ripin, D. J. & Goldberg, L. High efficiency side-coupling of light into optical fibres using imbedded v-grooves. *Electron. Lett.* **31**, 2204-2205 (1995).

7. Jauregui, C., Böhme, S., Wenetiadis, G., Limpert, J. & Tünnermann, A. Side-pump combiner for all-fibre monolithic fibre lasers and amplifiers. *JOSA B* **27**, 1011-1015 (2010).

8. Theeg, T., Sayinc, H., Neumann, J., Overmeyer, L. & Kracht, D. Pump and signal combiner for bi-directional pumping of all-fibre lasers and amplifiers. *Opt. Express* **20**, 28125-28141 (2012).

9. Abedin, K. S. et al. Multicore Erbium Doped Fibre Amplifiers for Space Division Multiplexing Systems. *J. Light. Technol.* **32**, 2800-2808 (2014).

10. Kim, K.-S. & Pratsinis, S. E. Manufacture of optical waveguide preforms by modified chemical vapor deposition. *AIChE J.* **34**, 912-921 (1988).

11. Geittner, P., Küppers, D. & Lydtin, H. Low-loss optical fibres prepared by plasma-activated chemical vapor deposition (CVD). Appl. Phys. Lett. 28, 645-646 (1976).

12. Izawa, T. & Inagaki, N. Materials and Processes for Fibre Preform Fabrication - Vapor-Phase Axial Deposition. *Proc. IEEE* **68**, 1184-1187 (1980).

13. Schultz, P. C. Fabrication of optical waveguides by the outside vapor deposition process. *Proc. IEEE* **68**, 1187-1190 (1980).

14. Townsend, J. E., Poole, S. B. & Payne, D. N. Solution-doping technique for fabrication of rare-earth-doped optical fibres. *Electron. Lett.* **23**, 329 (1987).

15. Sen, R. et al. Erbium Doped Optical Fibres-Fabrication Technology. *J. Opt.* **33**, 257-275 (2004).

16. Laegsgaard, J. & Bjarklev, A. Microstructured Optical Fibres-Fundamentals and Applications. *J. Am. Ceram. Soc.* **89**, 2-12 (2006).

17. Russell, P. Photonic crystal fibres. *Science* **299**, 358-62 (2003).

18. Dhar, A. et al. Characterization of porous core layer for controlling rare earth incorporation in optical fibre. *Opt. Express* **14**, 9006-9015 (2006).

19. Tang, F. Z., McNamara, P., Barton, G. W. & Ringer, S. P. Multiple solution-doping in optical fibre fabrication I - Aluminum doping. *J. Non-Cryst. Solids* **354**, 927-937 (2008).

20. Huang, B. et al. All-fibre mode-group-selective photonic lantern using graded-index multi-mode fibres. *Opt. Express* **23**, 224-234 (2015).

21. Guan, B., Ercan, B., Fontaine, N. K., Scott, R. P. & Yoo, S. J. B. Mode-Group-Selective Photonic Lantern based on Integrated 3D Devices Fabricated by Ultrafast Laser Inscription. in *Optical Fibre Communication Conference* W2A.16 (2015).

22. Winzer, P., Chen, H., Ryf, R., Guan, K. & Randel, S. Mode-dependent loss, gain, and noise in MIMO-SDM systems. in *40$^{th}$ European Conference and Exhibition on Optical Communication* (ECOC 2014) Mo.3.3.2 (2014).